

FORMATION OF MULTI-WALLED CARBON NANOTUBES AND GRAPHENE IN METHANE ARC DISCHARGE PLASMA

K. T. CHAUDHARY^{a*}, K. A. BAHTTI^b, M. S. RAFIQUE^b, H. JAMIL^b, J ALI^a, P. P. YUPAPIN^c, O. SAKTIOT^a, N BIDIN^a

^a*Institute of Advanced Photonics Science (APSI), Nanotechnology Research Alliance, Universiti Teknologi Malaysia, 81310, Johor Bahru, Malaysia.*

^b*Physics Department, University of Engineering and Technology, Lahore, Pakistan.*

^c*Nanoscale Science and Research Alliance (N'SERA), Faculty of Science, King Mongkut's Institute of Technology Ladkrabang, Bangkok 10520, Thailand.*

The growth of multi-walled carbon nanotube (MWCNT) and carbon nano structures is investigated in methane (CH₄) environment at low pressure using arc discharge process for arc currents 50, 70 and 90A. Plasma density and temperature are estimated by optical emission spectroscopy to determine the contribution of arc current and ambient environment towards the growth of MWCNT and nano structures. The grown samples at different arc currents are analyzed by transmission electron microscopy, scanning electron microscopy, Raman spectroscopy, Fourier Transform Infrared spectroscopy, thermogravimetric analysis and x-ray diffraction. An improvement in structure quality in term of defects and increase growth of MWCNT is observed in CH₄ ambient environment with increase in arc current. For arc current 90A, the well aligned and straight MWCNT along with graphene are detected.

(Received December 12, 2013; Accepted October 2, 2014)

Keywords: Electric Discharge; Arc Plasma Temperature & Density; Carbon Nanotubes

1. Introduction

The carbon nano materials are the center of attention due to their unique structure, properties and prospects for applications such as nanodevices, nanoelectronics, energy conversion devices, supercapacitors, non-volatile memory devices, hydrogen storage, flat-panel displays, material strengthening, micro- and nano-electromechanical systems[1-4]. The carbon nanomaterials contain incredible versatility in their structure and dimensions which attribute them unique properties such as mechanical strength, electrical conductivity and thermal or optical properties[3, 5, 6]. Various techniques have been developed for the growth of carbon nanotubes and nanomaterials such as arc discharge, chemical vapor deposition (CVD) and laser ablation[5, 7, 8]. All synthesis methods contain three major ingredients carbon source, catalyst nanoparticles and energy input. In the case of solid carbon source the synthesis method is high temperature method which involves the sublimation of solid source. Whereas for carbon source in liquid or gaseous phases, the synthesis methods are medium or low temperature methods[5]. Numerous studies on synthetic techniques e.g. arc discharge and catalytic chemical vapor deposition (CCVD) to grow high purity carbon nanotubes have been done[9]. Among several developed methods for the growth of carbon nano structures, arc discharge is the flexible and promising technique to yield highly graphitized carbon nanotubes and nano structures with fewer structural defects due to the very high temperature of arc plasma which provides suitable environment for the growth of carbon nanotubes and nano materials[4, 6, 10]. In arc discharge process a mixture of nanotubes with different structures i.e. diameter and chiral angle is produced and sorting of these different

* Corresponding Author: kashif.ali02@gmail.com

nanotubes is difficult task. In ideal condition, the carbon nanotubes features (diameter, chirality, defects, length) and location should be controlled directly at the synthesis stage which is not achieved yet due to the complexity of the process and phenomenon involves in growth of nanotubes[5]. Therefore, the control growth of carbon nanotube and nano structure is still an unresolved issue by arc discharge method[11]. In spite of long-standing efforts the gray areas persist in understanding the growth mechanisms[5]. High influx of plasma species and high temperatures play key role in the growth of nano structures. In order to realize and optimize the application of carbon nanotubes, the contribution of physical parameters such as ambient gas and pressure, electrode geometry, input power, gas flow, inter electrode distance, dynamics of plasma species etc. [6, 9] towards the growth of nanotubes and structures is need to explored and understand.

The hydrocarbon gases are widely used as precursor to grow the carbon nanotubes using CVD and plasma enhanced chemical vapor deposition (PCVD) techniques [11-13]. In this investigative work, the synthesis of multi-walled carbon nanotubes (MWCNT) by arc discharge process in methane (CH_4) environment for different applied arc currents is studied to exploit the potential of CH_4 towards the growth and structure of MWCNT. The CH_4 gas serves as source of carbon and hydrogen, as the good quality MWCNT are synthesized in hydrogen environment [11]. The plasma temperature and density are determined for different input powers by in situ optical emission spectroscopy. The synthesized MWCNT for different input powers are analyzed by microscopic and spectroscopic techniques to explore the influence of arc current and ambient gas on the growth and structure quality of carbon nano structures.

2. Experimental

The arc discharge is produced between two 4N graphite rods in CH_4 environment at lower pressure 500torr for arc current 50, 70 and 90A. The solid graphite rod with diameter 11mm is used as cathode whereas the hollow graphite rod with outer diameter 6mm and inner diameter 4 mm is used as anode. The optical spectra of arc plasma generated at different applied arc currents are recorded for integration time 300ms using Ocean Optics HR4000, 200-650nm, 0.1nm in optical range 300-650nm. By using bi-convex lens of focal length 15cm, the radiations are focused into the optical fiber of diameter 600 μm connected to the optical spectrometer. The MWCNT samples synthesized at different experimental conditions are collected from cathode deposit and characterized by transmission electron microscopy (TEM), scanning electron microscopy (SEM), x-ray diffraction (XRD) analysis, Raman spectroscopy, Fourier Transform Infrared (FTIR) spectroscopy and thermogravimetric analysis (TGA) to investigate structure, quality and thermal stability of the grown carbon nanotubes.

3. Results & Discussion

3.1 Optical Emission Spectral Analysis

The arc discharge is initiated by bringing the graphite electrodes in contact and then separated immediately. The combined effect of the high current density and relatively high resistance of the individual contact spots causes localized heating and rise the temperature of the connected surfaces, which vaporizes the material at the contact areas and causes the sublimation of graphite anode. The plasma temperatures and densities are calculated by in situ optical emission spectroscopy[5] for applied arc current 50, 70 and 90A at ambient pressures 500torr with CH_4 as feedstock & background gas. As inside the arc plasma, the dynamics is governed by the applied electric field associated to input power and pressure gradient[12, 13]. The spectral line at different position in spectra are observed with change in arc current due to change in the dynamics of the plasma species. From the captured optical spectra, the spectral lines corresponding to neutral carbon atoms (CI 473.4 & 473.5nm), singly ionized carbon ions (CII 358.4, 426.7 & 553.5nm) and doubly ionized carbon ions (CIII 388.3, 415.2 & 467.3nm) are used to determine the plasma

temperature and density of the corresponding species in the carbon arc plasmas. The processed recorded spectra for arc current 50, 70 and 90A in CH₄ ambient environment at pressures 500torr with labeled peaks are given in Figure 1.

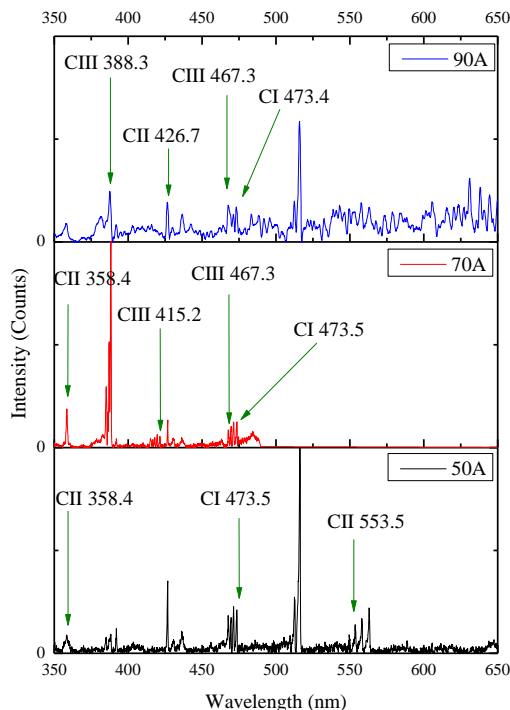


Fig. 1. Optical emission spectra of arc plasma for arc currents 50, 70 and 90A

The plasma temperature and densities for applied arc currents are estimated by Boltzmann intensity ratio method (as given in Eq. 1) and Saha equation (as given in Eq. 2) respectively [12] under the special circumstances of local thermodynamic equilibrium (LTE), which is tested according to McWhirter's Criterion [12].

$$T = - \frac{E_i - E_m}{k \ln \left(\frac{I_{ij} \lambda_{ij} A_{mn} \varpi_m}{I_{mn} \lambda_{mn} A_{ij} \varpi_i} \right)} \quad (1)$$

where ' T ' is the plasma temperature, E_i & E_m are the higher level energies of two different transitions of same ionization state as either CII or CIII, λ_{ij} & λ_{mn} are the emitted wavelengths, A_{ij} & A_{mn} are the transition probabilities of higher level, ϖ_i & ϖ_m are the degeneracies, I_{ij} & I_{mn} are the intensities of emitted wavelengths and k is the Boltzmann constant.

$$n_e = \frac{2(2\pi m_e kT)^{3/2}}{h^3} \frac{I^i \lambda^i A^{i+1} \varpi^{i+1}}{I^{i+1} \lambda^{i+1} A^i \varpi^i} e^{-\frac{(E^{i+1} - E^i + \chi_i)}{kT}} \quad (2)$$

Where n_e is the plasma density, m_e is the mass of electron T is the plasma temperature, E^{i+1} , & E^i are the higher level energies of singly ionized carbon atom (CII) and neutral carbon atom (CI) respectively, χ^i is the first ionization energy of carbon, λ^{i+1} & λ^i are the emitted wavelengths by CII and CI species, A^{i+1} & A^i are the transition probabilities of higher level for CII and CI, ϖ^{i+1} & ϖ^i are the degeneracy of the higher energy levels for CII and CI, I^{i+1} & I^i are the intensities of emitted spectral lines, h is the Planck's constant and k is the Boltzmann constant.

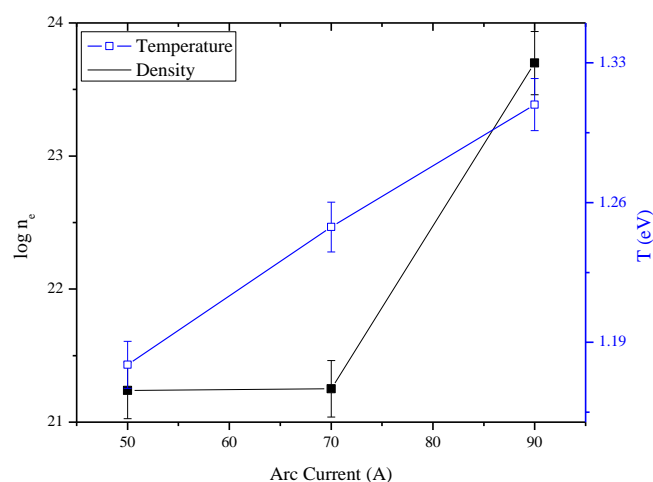


Fig. 2. Plasma density and temperature for arc current 50, 70 and 90A

The estimated values of the plasma temperatures and densities for arc currents 50, 70 and 90A are plotted graphically in Figure 2. A linear increase in plasma temperature with increase in arc current is observed. The plasma density is found in the range of 1.73×10^{21} to $5.0 \times 10^{23} \text{ cm}^{-3}$ as arc current increases for 50 to 90A. A small increase in the plasma density is observed with increase in arc current from 50 to 70A however, a rapid increase in the plasma density [4, 6] is observed for further increase in the arc current from 70 to 90A as depicted in Figure 2. The increase in applied arc current increases the energy flux at the anode surface and arc radius which in turn enhances the ablation of the anode and accelerates the ablation of anode [14]. During arc discharge the CH_4 molecules decompose into carbon and hydrogen [15]. The increase in the arc current enhances the decomposition and ionization of residence gas and as a result provides more carbon species within the plasma volume.

3.2 Analysis of Grown MWCNT and Nano structures

The synthesized samples are analyzed by JEM-2100, 200kV class TEM with probe size 0.5nm. For the TEM analysis, the specimens are prepared by sonication of synthesized sample material in ethanol for 15 minutes. The closed end MWCNT along with different carbon nano structures such as carbon nano capsules, carbon onion and graphene flakes are observed as shown in Figure 3. The MWCNT are found with outer diameter $< 20 \text{ nm}$ and inner diameter $< 10 \text{ nm}$ as shown in Figure 3(a, b and c). The carbon nano structures as nano-capsule with diameter $\sim 10 \text{ nm}$ and nearly spherical nano onion with diameter $\sim 35 \text{ nm}$ and graphene are also spotted as illustrated in Figure 3(d, e and f). The inter-wall spacing in observed MWCNT and carbon nano structures is determined in the range of 0.34nm. For higher arc current 90A fully developed MWCNT with fewer defects are observed as compared to the MWCNT grown for lower arc current i.e. 50 and 70A as shown in Figure 3(a and b).

From TEM microscopic analysis, the improvement in the wall alignment and growth rate is observed with increase in the arc current from 50 to 90A. For higher arc current the temperature of cathode surface is higher which anneals the poorly aligned tubular structures and leads to formation of fully developed well aligned MWCNT. However, for high arc current, increase in the growth of nano structures and graphene is also observed.

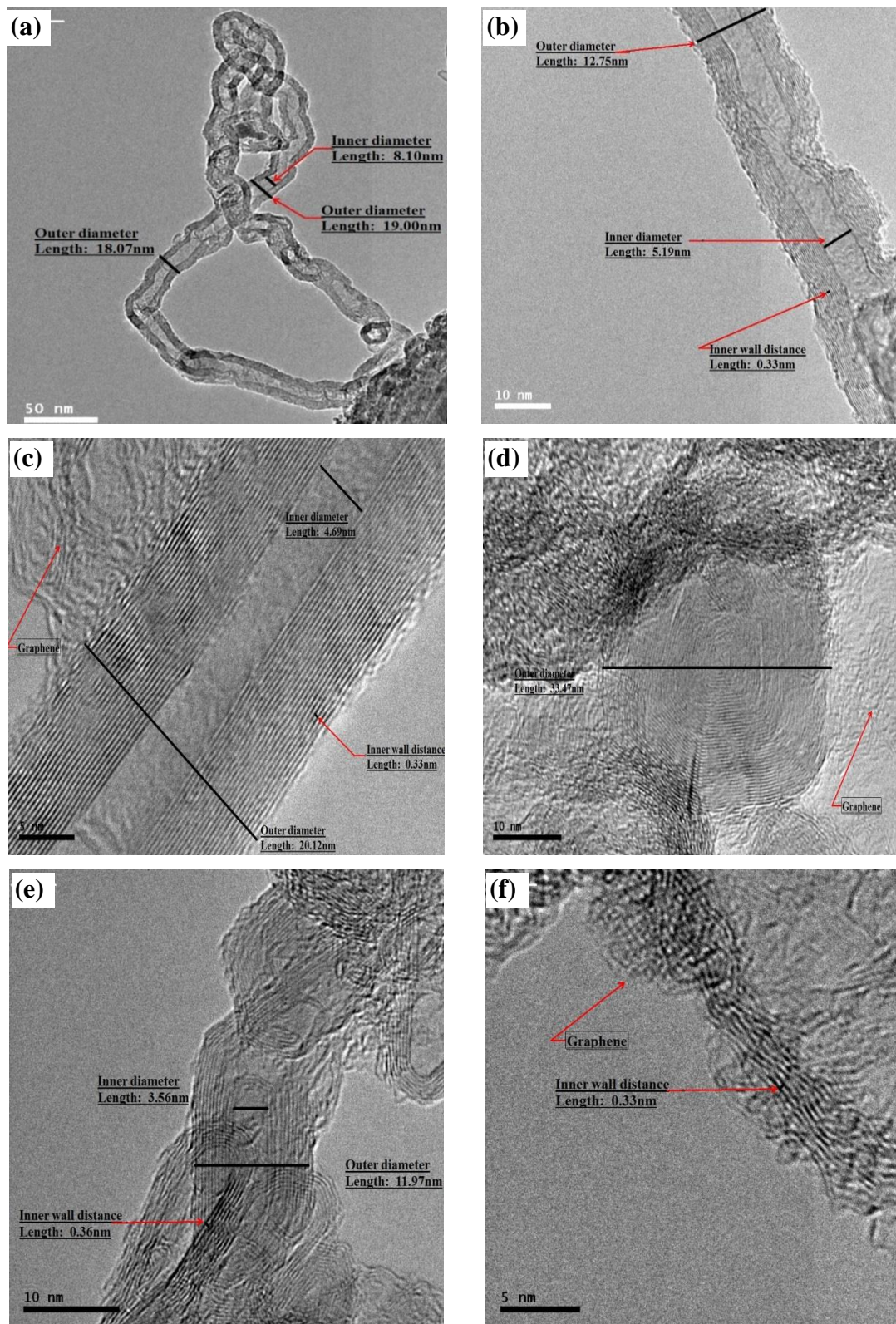


Fig. 3. Transmission electron micrographs of synthesized MWCNT for arc current (a) 50A, (b) 70A and (c-f) 90A

Fig. 4 shows the XRD spectra of MWCNT samples grown for arc current 50, 70 and 90A. The strong peak for plane (002) and low intensity peaks for planes (100), (101), (004) at position $\sim 26^\circ$, 42° , 44° and 54° respectively for angle 2θ are observed [16]. XRD characterization are carried out by Siemens D5000 Diffractometer for x-rays of wavelength 1.54\AA . The recorded XRD spectra

are processed and characterized using Eva Diffrac Plus software. The strong peaks at $\sim 26.5^\circ$ correspond to the (002) graphite plane indicate the presence of strong graphitized structures in all prepared samples.

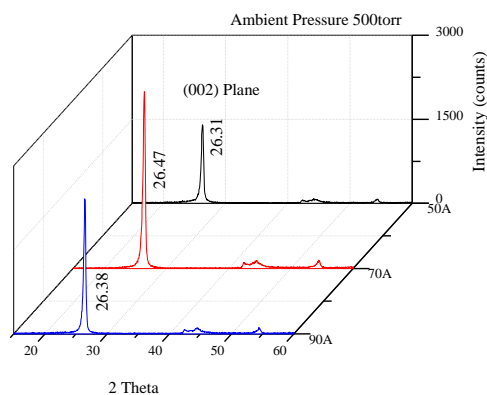


Fig. 4. XRD Spectra of synthesized MWCNT for arc current 50A, 70A, 90A

The Fig. 5 shows the d-spacing profile of synthesized MWCNT with increase in the arc current from 50 to 90A. The d-spacing is found in range of 0.336 to 0.340 nm which is higher than the graphitic lattice and is consistent with the TEM micrographs in which the average distance between the outer walls of MWCNTs is 0.34nm. The higher value of d-spacing is observed for MWCNT grown for arc current 90A, which shows the increase in the growth of MWCNT with small diameter, as the interwall spacing for MWCNT with small diameter is higher [17].

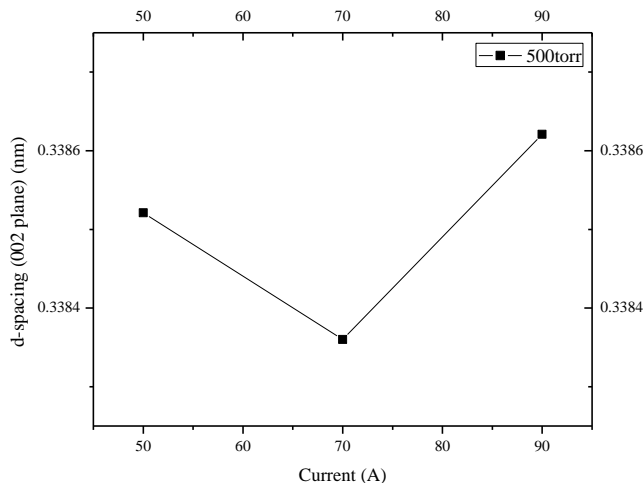


Fig. 5. Variation in d-spacing of MWCNT synthesized for arc current 50, 70 and 90A

The asymmetry in the (002) peak profile is due to the presence of the different carbon nano crystalline structures and defective sites of ill-organized nanotubes as observed in TEM micrographs. The presence of peak at about $2\theta=43.3^\circ$ in all XRD spectra shows the presence of hexagonal ring structure [18].

The synthesized MWCNT are analyzed by JEOL SEM operated in range of 10kV to 15kV. The randomly oriented carbon nanotubes with high aspect ratios and density along with nano particles, amorphous carbon, graphene flakes are observed.

Figures 6(a, b and c) shows the scanning electron microscopic images of the synthesized MWCNT sample for arc current 50, 70 and 90A respectively. An increase in density and growth of carbon nanotubes is observed with increase in arc current from 50 to 90A. However, beside the

enhancement in the growth of carbon nanotubes, an increase in the growth of graphene flakes is also detected for higher value of arc current as shown in Figure6(c).

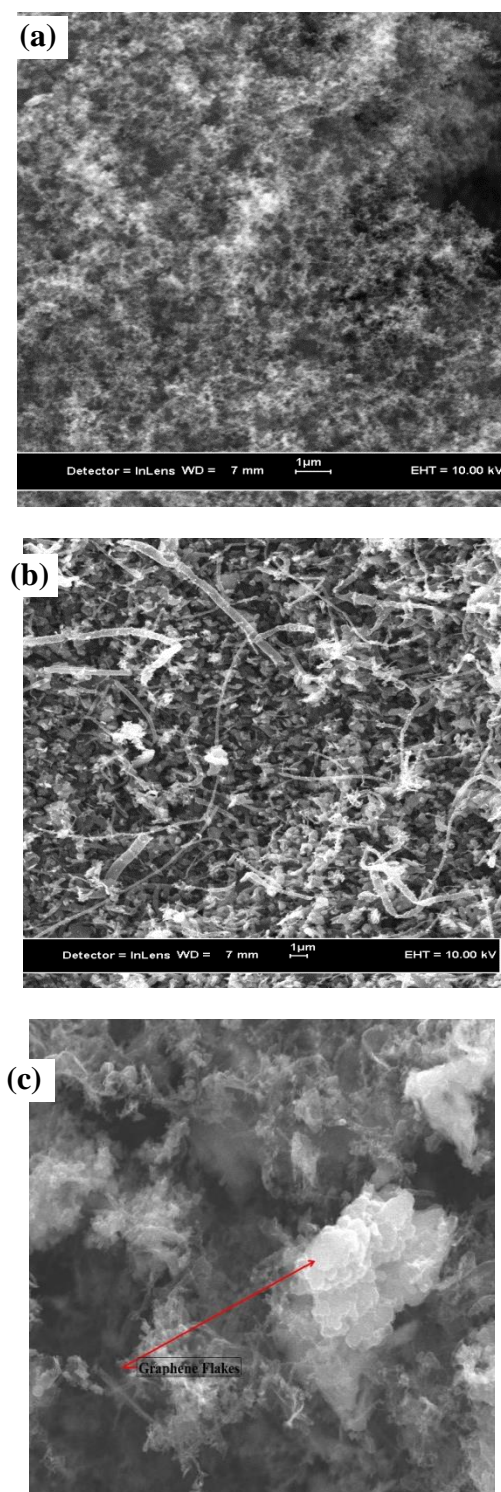


Fig. 6. Scanning electron micrographs of MWCNTs synthesized at ambient pressure 500 torr for arc current (a) 50A, (b) 70A and (c) 90A

Raman spectroscopic analysis is performed for synthesized MWCNT samples using HORIBA Jobin Yvon's Modular Raman spectrometer equipped with He-Ne laser of wavelength 632.8nm and energy 14.7mW in frequency range 200 to 3750 cm^{-1} . The spectral lines in region of

1325 to 1330 cm^{-1} , 1580 to 1590 cm^{-1} and 2630 to 2680 cm^{-1} named as D-line, G-line and G'-line respectively are observed in all recorded Raman spectra of MWCNT samples as shown in Figure 7.

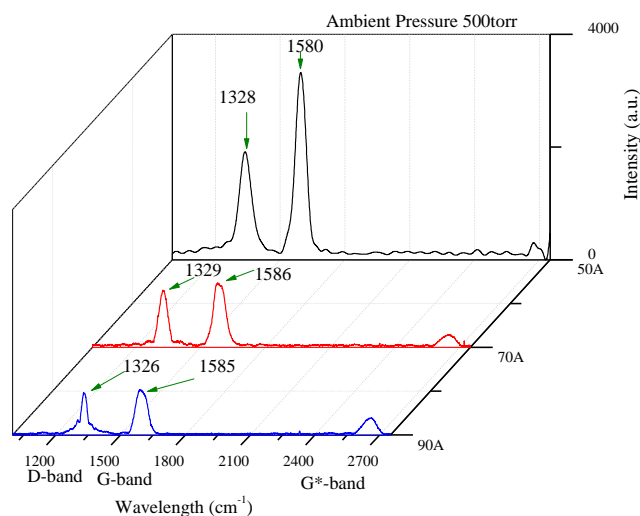


Fig. 7. Raman spectra of synthesized MWCNT for arc current 50, 70 and 90A

The strongest G-line in the region of 1580 to 1590 cm^{-1} identifies the presence of highly graphitized nano tubes and structures in the grown samples. The high intensity D-line in the region of 1325 to 1330 cm^{-1} refers the presence of poorly organized graphitic structures. However, D-line is also considered as intrinsic feature of MWCNT Raman spectrum because the curved nature of the graphite sheets increases the intensity of D-line due to enhancement in the electron-phonon coupling [19]. The G'-band shows the presence of the crystalline graphite in form of one or multilayer of graphene [20] in the samples as observed in TEM microscopy. It is observed that the intensity of D-line relative to intensity of G-line is increased with increase in arc current. The increase in the intensity of D-line can be attribute presence of defective structure and increase in the growth of carbon nanotubes with smaller diameter and carbon nanostructures such as carbon onions, capsules, which is in agreement with the transmission electron microscopic analysis. An increase in the relative intensity of the G'-line with respect to G-line is also observed as depicted in Figure 7. The relative increase in the G'-line intensity illustrates the enhancement in the growth of graphene [21, 22] as arc current increases. Figures 8(a and b) show the shift in D and G-lines respectively with respect to arc current.

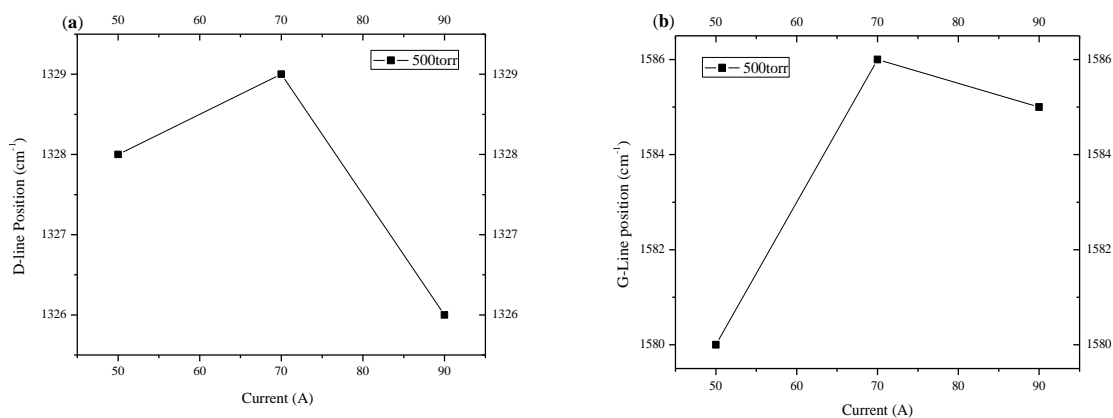


Fig. 8: Variation in (a) D- and (b) G- line positions with respect to arc current

A downshift in D -line positions at higher arc current and upshift in G-line with increase in arc current is observed. The downshift in D-line at higher arc current indicates rise in the growth of MWCNT with small diameter and increase in the growth of graphene flakes[23]. The upshift of G-line shows the increase in the growth of nano structures. Figure 9 presents the variation in the intensity ratio of D-line and G-line with respect to arc current respectively. An increase in the values of I_D/I_G ratio are obtained for the synthesized MWCNT samples with increase in the arc current, which indicate the presence of amorphous carbon, nano crystallites and graphene stacks. The Raman spectral analysis of synthesized MWCNT samples infer an improvement in the structure of the carbon nanotubes and increase in the growth of the graphite crystallite and graphene with increase applied arc current. The downshift in D -line position with increase in the arc current represents the improvement in structural quality of grown MWCNT. However, the high I_D/I_G ratios show that the synthesized samples contain the MWCNT along with graphite crystallites, carbon nanostructures and amorphous carbon.

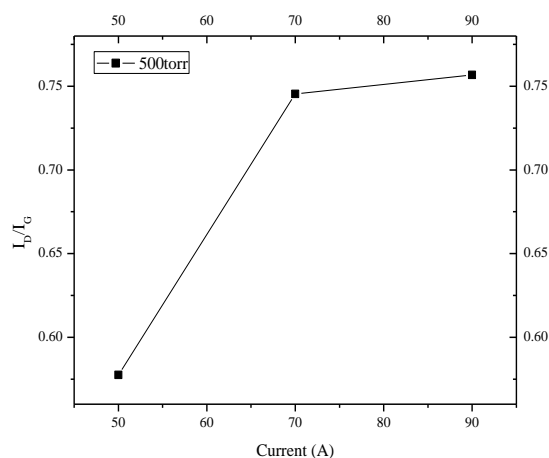


Fig. 9. Variation in intensity ration of D and G lines with respect to arc current

Figure 10 shows FTIR spectra of MWCNT prepared for arc current 50, 70 and 90A. The samples for the FTIR spectroscopy are prepared by grinding the MWCNT material (powder) with 300mg potassium bromide (KBr) and pressed into to pellet of diameter 1 cm by applying load of 10 tons for 1minute. The Perkin Elmer Instruments Spectrum one FTIR spectrometer equipped with KBr detector and controlled by spectrum V5.3.1 software is used. Each recorded spectrograph is the average of 10 scans in the range of 400 to 4000 cm^{-1} .

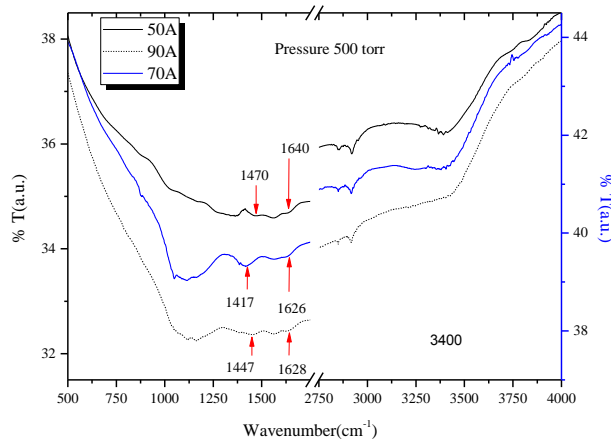


Fig. 10: FTIR spectra of synthesized MWCNT for arc current 50A, 70A and 90A

The spectral peaks in the the region of $1560\text{-}1580\text{cm}^{-1}$ and at 1460cm^{-1} represents the C–C vibrational modes associate to the carbon skeleton of the MWCNT [24-27]. The vibration at $\sim 1620\text{cm}^{-1}$ refere to the presence of C=C group [28].

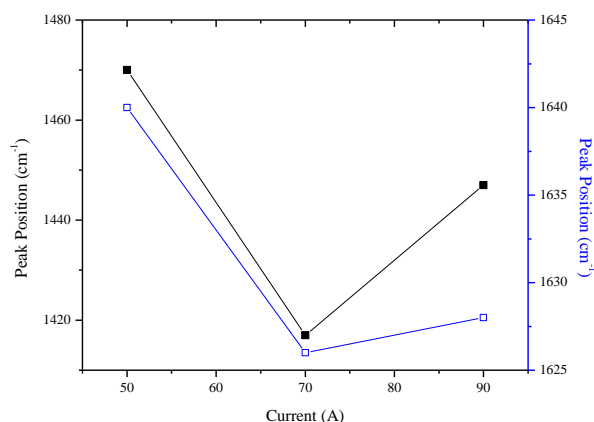


Fig. 11: Variation in peak at positions 1440cm^{-1} and 1635cm^{-1} with respect to applied arc current.

Fig. 11 shows variation in peaks at positions 1450cm^{-1} and 1635cm^{-1} . The broadening and downshift in spectral lines associated to C–C stretching mode at 1450cm^{-1} and C=C stretching mode at $\sim 1635\text{cm}^{-1}$ is observed with increase in arc current. The downshift and broadening in the peak associated to C–C stretching mode indicates the increase in the growth of the carbon nano tubes and carbon nano structure with increase in applied arc currents. The downshift in the peaks shows the presence of nano structures with curved surfaces, finite size and presence carbon species of various bond lengths. The broadening in the peaks corresponds to the relative abundance of the nano structures with different dimensions in sample materials prepared at different experimental conditions.

The thermal gravimetric analysis (TGA) of grown MWCNT is performed by PerkinElmer Paris 1 system to calculate the weight loss percentage and decomposition temperature. Figure 12 shows the result of TGA test for grown MWCNT. The decomposition temperature is found at point 572°C .

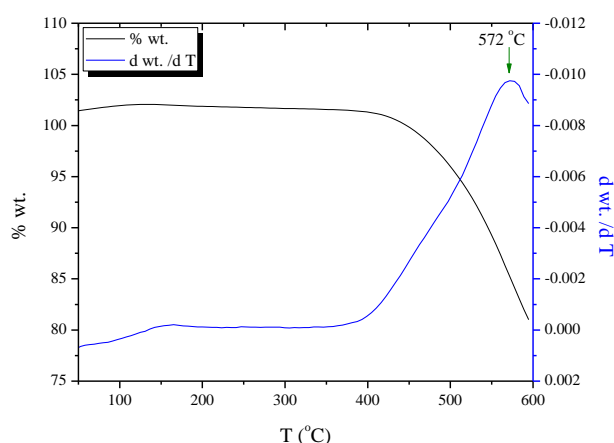


Fig. 12: Thermogravimetric (TGA) percentage weight loss and 1st derivative curves with respect to temperature

Form Figure 12, it is observed that only 20% sample material is decompsed upto temperature 600°C , which shows the high thermal stabilty and presence of MWCNT as major product in the sample material [29, 30]. The initiation temperature for the sample material is found

in the region of 400 to 425 °C, which shows the presence of the amorphous carbon and other nano structures i.e. nano onions and nano particles as observed in electron microscopic characterization.

From different analysis of the grown MWCNT, It is observed that the structural quality of grown MWCNT is improved with increase in the arc current from 50 to 90A. The higher arc discharge current raises the temperature of the cathode surface, which anneals the poorly oriented nanotube structures into properly aligned MWCNT. During the arc discharge process, the CH₄ molecules decompose and ionized and serve as feedstock and enhance the cathode deposit which in turn increases the growth of carbon nanotubes. The growth of graphene can attribute to the presence of hydrogen which eliminates due of dissociation of CH₄ molecules [31].The atomic hydrogen coupled with incident carbon ions on the cathode surface and ceased the formation of closed structures which in turn leads to the increase in yield of graphene.

4. Conclusion

The closed end MWCNT with tube diameter <20nm along with other nanostructures as onions, capsules, nano particles, amorphous carbon and graphene are grown by arc discharge process in CH₄ environment at pressures 500torr for arc currents 50, 70 and. An increase in the growth and improvement in the structure quality of nanotubes in term of defects and alignment is observed with increase in the arc current. For arc current 90A, the high temperature of cathode surface provides sufficient temperature conditions to anneal the nano structures and leads to formation well aligned tube structures.

Acknowledgement

We would like to thank the Institute of Advanced Photonics Science, Nanotechnology Research Alliance, Universiti Teknologi Malaysia (UTM), Unviversity of Engineering & Technology (UET) Lahore Pakistan and King Mongkut's Institute of Technology (KMITL), Thailand for providing research facilities. This research work has been supported by FRGS (R.J130000.7809.4F519) Grant.

References

- [1] O. Volotskova, I. Levchenko, A. Shashurin, Y. Raitses, K. Ostrikov, M. Keidar, *Nanoscale* **2**(10), 2281 (2010).
- [2] M. Corrias, P. Serp, P. Kalck, G. Dechambre, J. Lacout, C. Castiglioni, Y. Kihn, *Carbon* **41**(12), 2361 (2003).
- [3] A. J. Fetterman, Y. Raitses, M. Keidar, *Carbon* **46**(10), 1322-1326 (2008).
- [4] M. Keidar, *Journal of Physics D: Applied Physics* **40**, 2388 (2007).
- [5] C. Journet, M. Picher, V. Jourdain, *Nanotechnology* **23**(14), 142001 (2012).
- [6] M. Keidar, A. M. Waas, *Nanotechnology* **15**, 1571 (2004).
- [7] K. Awasthi, A. Srivastava, O. Srivastava, *Journal of nanoscience and nanotechnology* **5**(10), 1616 (2005).
- [8] J. Prasek, J. Drbohlavova, J. Chomoucka, J. Hubalek, O. Jasek, V. Adam, R. Kizek, *Journal of Materials Chemistry* **21**(40), 15872 (2011).
- [9] Y. A. Kim, H. Muramatsu, T. Hayashi, M. Endo, *Carbon* **50**(12), 4588 (2012).
- [10] M. Keidar, A. Shashurin, O. Volotskova, Y. Raitses, I. I. Beilis, *Physics of Plasmas* **17**(5), 057101 (2010).
- [11] X. Cai, H. Cong, C. Liu, *Carbon* **50**(8), 2726 (2012).
- [12] R. Noll, *Laser-Induced Breakdown Spectroscopy: Fundamentals and Applications*. Springer-Verlag Berlin Heidelberg (2012).
- [13] H. O. Pierson, *Handbook of Carbon, Graphite, Diamond and Fullerenes: Properties,*

- Processing and Applications. Noyes Publications. 399 (1993).
- [14] M. Keidar, I. Beilis, *Journal of Applied Physics* **106**(10), 1033041 (2009).
- [15] K. Shimotani, K. Anazawa, H. Watanabe, M. Shimizu, *Applied Physics A: Materials Science & Processing* **73**(4), 451 (2001).
- [16] Y. Sun, S. Yang, G. Sheng, Z. Guo, X. Wang, *Journal of environmental radioactivity* **105**, 40 (2012).
- [17] Z. Li, C. Lu, Z. Xia, Y. Zhou, Z. Luo, *Carbon* **45**(8), 1686 (2007).
- [18] G. Onyestyák, J. Valyon, K. Hernadi, I. Kiricsi, L. Rees, *Carbon* **41**(6), 1241-1248 (2003).
- [19] J. Sengupta, C. Jacob, *Journal of Nanoparticle Research* **12**(2), 457-465 (2010).
- [20] L. Cancado, K. Takai, T. Enoki, M. Endo, Y. Kim, H. Mizusaki, N. Speziali, A. Jorio, M. Pimenta, *Carbon* **46**(2), 272-275 (2008).
- [21] M. Endo, Y. Kim, T. Takeda, S. Hong, T. Matusita, T. Hayashi, M. Dresselhaus, *Carbon* **39**(13), 2003 (2001).
- [22] A. Gupta, G. Chen, P. Joshi, S. Tadigadapa, P. Eklund, *Nano Letters* **6**(12), 2667 (2006).
- [23] D. Graf, F. Molitor, K. Ensslin, C. Stampfer, A. Jungen, C. Hierold, L. Wirtz, *Nano letters* **7**(2), 238 (2007).
- [24] L. Liu, Y. Qin, Z.-X. Guo, D. Zhu, *Carbon* **41**(2), 331 (2003).
- [25] Y.-H. Li, C. Xu, B. Wei, X. Zhang, M. Zheng, D. Wu, P. Ajayan, *Chemistry of materials* **14**(2), 483 (2002).
- [26] L. Yan, P. R. Chang, P. Zheng, *Carbohydrate Polymers* **84**(4), 1378 (2011).
- [27] H. Naeimi, A. Mohajeri, L. Moradi, A. M. Rashidi, *Applied Surface Science* **256**(3), 631 (2009).
- [28] S. Y. Sawant, R. S. Somani, H. C. Bajaj, S. S. Sharma, *Journal of hazardous materials* **227-228**, 317 (2012).
- [29] J. H. Lehman, M. Terrones, E. Mansfield, K. E. Hurst, V. Meunier, *Carbon* **49**(8), 2581 (2011).
- [30] L. S. Pang, J. D. Saxby, S. P. Chatfield, *The Journal of Physical Chemistry* **97**(27), 6941 (1993).
- [31] Z. Wang, N. Li, Z. Shi, Z. Gu, *Nanotechnology* **21**(17), 175602 (2010).